

Automatic retinal blood flow calculation using spectral domain optical coherence tomography

Hassan Wehbe^{1,2}, Marco Ruggeri¹, Shuliang Jiao¹, Giovanni Gregori¹
Carmen A. Puliafito¹ and Weizhao Zhao²

¹Bascom Palmer Eye Institute, University of Miami Miller School of Medicine, 1638 NW 10th Ave, Miami, FL 33136

²Department of Biomedical Engineering, University of Miami, Coral Gables, FL 33124-0621

sjiao@med.miami.edu; <http://www.bpei.med.miami.edu>

Abstract: Optical Doppler tomography (ODT) is a branch of optical coherence tomography (OCT) that can measure the speed of a blood flow by measuring the Doppler shift impinging on the probing sample light by the moving blood cells. However, the measured speed of blood flow is a function of the Doppler angle, which needs to be determined in order to calculate the absolute velocity of the blood flow inside a vessel. We developed a technique that can extract the Doppler angle from the 3D data measured with spectral-domain OCT, which needs to extract the lateral and depth coordinates of a vessel in each measured ODT and OCT image. The lateral coordinates and the diameter of a blood vessel were first extracted in each OCT structural image by using the technique of blood vessel shadowgram, a technique first developed by us for enhancing the retinal blood vessel contrast in the *en face* view of the 3D OCT. The depth coordinate of a vessel was then determined by using a circular averaging filter moving in the depth direction along the axis passing through the vessel center in the ODT image. The Doppler angle was then calculated from the extracted coordinates of the blood vessel. The technique was applied in blood flow measurements in retinal blood vessels, which has potential impact on the study and diagnosis of blinding diseases like glaucoma.

©2007 Optical Society of America

OCIS codes: (110.4500) Optical coherence tomography; (120.3890) medical optics instrumentation; (170.4580) optical diagnostics for medicine.

References and links

1. J. Flammer, S. Orgül, V. P. Costa, N. Orzalesi, G. K. Kriegelstein, L. M. Serra, J. P. Renard, and E. Stefánsson, "The impact of ocular blood flow in glaucoma," *Prog. Retinal Res.* **21**, 359–393 (2002).
2. R. Allingham, K. Damji, S. Freedman, S. Moroi, G. Shafranov, M. Shields, *Shields' textbook of glaucoma*, Fifth Edition, (Lippincott Williams & Wilkins, 2005).
3. E. Dienstbier, J. Balik and H. Kafka, "A contribution to the theory of the vascular theory of glaucoma," *Br. J. Ophthalmol.* **34**, 47–58 (1950).
4. H. Ren, K. M. Brecke, Z. Ding, Y. Zhao, J. S. Nelson, and Z. Chen, "Imaging and quantifying transverse flow velocity with the Doppler bandwidth in a phase-resolved functional optical coherence tomography," *Opt. Lett.* **27**, 409–411 (2002).
5. T. G. van Leeuwen, M. D. Kulkarni, S. Yazdanfar, A. M. Rollins, and J. A. Izatt, "High-flow-velocity and shear-rate imaging by use of color Doppler optical coherence tomography," *Opt. Lett.* **24**, 1584–1586 (1999).
6. H. Wehbe, M. Ruggeri, S. Jiao, G. Gregori, C. Puliafito "Automatic retinal blood vessel parameter calculation in spectral domain optical coherence tomography," *Proc. SPIE*, **6429** 64290D (2007).
7. V. X. D. Yang, M. L. Gordon, A. Mok, Y. Zhao, Z. Chen, R. Cobbold, B. Wilson, and I. Vitkin, "Improved phase resolved optical Doppler tomography using the kasai velocity estimator and histogram segmentation," *Opt. Commun.* **208**, 209–214 (2002).
8. J. Schuman, T. Pedut-Kloizman, E. Hertzmark, M. Hee, J. Wilkins, J. Coker, C. Puliafito, J. Fujimoto, and E. Swanson "Reproducibility of nerve fiber layer thickness measurements using optical coherence Tomography," *Ophthalmol.* **103**, 1889–1898 (1996).

9. E. Blumenthal, J. Williams, R. Weinreb, C. Girkin, C. Berry, "Reproducibility of Nerve Fiber Layer Thickness Measurements by use of Optical Coherence Tomography," *Ophthalmol.* **107**, 2278-2282 (2000).
10. V. Guedes, J. Schuman, E. Hertzmark, G. Wollstein, A. Correnti, R. Mancini, D. Lederer, S. Voskarian, L. Velazquez, H. Pakter, T. Pedut-Kloizman, J. G. Fujimoto, C. Mattox, "Optical Coherence Tomography Measurement of Macular and Nerve Fiber Layer Thickness in Normal and Glaucomatous Human Eyes," *Ophthalmol.* **110**, 177-189 (2003).
- S. Jiao, R. Knighton, X. Huang, G. Gregori, and C. A. Puliafito, "Simultaneous acquisition of sectional and fundus ophthalmic images with spectral-domain optical coherence tomography," *Opt. Express* **13**, 444-452 (2005).
11. A. Weber, M. Cheney, Q. Smithwick, and A. Elsner, "Polarimetric imaging and blood vessel quantification," *Opt. Express* **12**, 5178-5190 (2004).
12. A. Yoshida, G. Feke, F. Mori, T. Nagaoka, N. Fujio, H. Ogasawara, S. Konno, and J. Mcmeel, "Reproducibility and clinical application of a newly developed stabilized retinal laser Doppler instrument," *Am. J. Ophthalmol.* **136**, 404-404 (2003).

1. Introduction:

Glaucoma is one of the leading causes of blindness in the world and is usually associated with increased intraocular pressure (IOP). There are two theories for the pathogenesis of glaucomatous optic neuropathy (GON): the mechanical and the vascular theory, both of which have been the debate subject of multiple research groups throughout the past 150 years. [1,2-3] The vascular theory considers GON to be the result of ischemia caused by the elevated IOP or other risk factors obstructing the blood flow. A tool providing accurate quantitative structural and blood flow information will benefit the study of the etiology of glaucoma as well as the developments of new therapies by monitoring the treatment effects non-invasively. Optical Doppler tomography (ODT) is a branch of optical coherence tomography (OCT) that can measure the spatially resolved speed of a blood flow by measuring the Doppler shift caused by the moving blood cells to the probing sample light. [4,5] The measured Doppler shift (f_d) is related to the velocity by:

$$f_d = \frac{2nv_a}{\lambda_0} \cos \theta, \quad (1)$$

where v_a is the absolute velocity of the moving blood cells, λ_0 is the center wavelength of the light source, n is the refractive index of the sample and θ is the Doppler angle. From the above equation it is clear that the calculated velocity from the measured Doppler shift is the projection of the absolute velocity on the direction of the incident probing light. Accordingly, in order to calculate the absolute velocity from the measured Doppler shift we need to know the Doppler angle θ . However θ is not only an unknown parameter in retinal ODT imaging but also changes at different imaging time.

Spectral-domain optical coherence tomography (SD-OCT) is a recently developed high speed OCT technology that provides high resolution three dimensional imaging of biological tissues. SD-OCT provides the means of calculating the Doppler angle from the acquired 3D data, which provides structural (3D orientations and the blood vessel diameters) and Doppler information of the retinal blood vessels. [6] In this paper we report on our study on the automatic extraction of the parameters of the retinal blood vessels from the images acquired with a high resolution high speed SD-OCT. The retinal blood flow can be calculated upon acquisition of these parameters together with the Doppler information.

2. Materials and methods

2.1 Ultra high resolution OCT system

A high-speed high resolution 3D SD-OCT was built for the investigation. In the SD-OCT system, the low-coherence light from a three-module superluminescent diode (T-840

Broadlighter, Superlum Diodes Ltd. Moscow, Russia) with center wavelength of 840 nm and FWHM bandwidth of 100 nm is coupled into an optical fiber-based Michelson interferometer. In the sample arm, the sample light is delivered to the retina by a modified optical head of an OCT 2 system (Carl Zeiss Meditec Inc., Dublin, CA). In the detection arm, a spectrometer consisting of a collimating lens, a transmission grating (1200 line/mm), a multi-element imaging lens ($f = 180$ mm), and a line scan CCD camera (Aviiva-SM2-CL-2014, 2048 pixels with 14 micron pixel size operating in 12-bit mode) was used to detect the combined reference and sample light. The calculated spectral resolution of the spectrometer was 0.055 nm, which corresponds to a detectable imaging depth range of 3.1 mm in air. The calibrated depth resolution in the tissue is $\sim 3\mu\text{m}$, which was corrected with the refractive index of biological tissues. The power of the sample light was lowered to $750\mu\text{W}$ by adjusting the source power to ensure that the light intensity delivered to the eye was within the ANSI standard. OCT scans consisting of a total number of 65536 depth scans (A-scans) takes 2.7 seconds.

2.2 Doppler imaging

The measured raw spectral interference signals were processed by using the standard algorithm for spectral domain OCT to get the complex signal $[\Gamma(t)]$ in the time domain. To calculate the Doppler shift we first calculated the product of the complex signals for the adjacent A-lines:

$$\Gamma_{i+1}(t) \bullet \Gamma_i^*(t) = A(t)e^{i[\varphi_{i+1}(t) - \varphi_i(t)]} \quad (2)$$

where $\Gamma^*(t)$ is the complex conjugate of $\Gamma(t)$; A is the amplitude of the product; φ_i is the phase of $\Gamma_i(t)$; i is the A-line number. The phase difference among the adjacent A-lines $\Delta\varphi_i = \varphi_{i+1} - \varphi_i$ can then be calculated. Calculating the phase difference with Eq. (2) has the advantage of avoiding the problem of phase unwrapping.

The projected flow speed on the direction of the incident sample light can be calculated from $\Delta\varphi_i$:

$$v_p = \frac{\Delta\varphi_i \lambda_0 f_{A\text{-line}}}{4\pi n}, \quad (3)$$

$$-\pi \leq \Delta\varphi_i \leq \pi, \quad -\frac{\lambda_0 f_{A\text{-line}}}{4n} \leq v_p \leq \frac{\lambda_0 f_{A\text{-line}}}{4n},$$

where v_p is the projection of the absolute velocity v_a along the depth direction, λ_0 is the center wavelength of the light source (840 nm), $f_{A\text{-line}}$ is the axial scan frequency (24000 A-lines/sec), n is the index of refraction of the sample (~ 1.4). Accordingly, the maximal speed that can be detected by our system without phase wrapping is ± 3.6 mm/sec.

The Doppler image contains bulk motion artifacts that is additive to the Doppler shift induced by the blood flow. Bulk motion effect can be quantified for each A-line by using the histogram technique [7]. Briefly speaking, the histogram $H(\Delta\varphi_i)$ of the phase difference $\Delta\varphi_i$ was calculated along each individual line of the Doppler image. $H(\Delta\varphi_i)$ contained N bins varying in the interval $[-\pi, \pi]$ with a step size of $\Delta\varphi_h = \frac{\Delta\varphi_{\max} - \Delta\varphi_{\min}}{N}$, where $\Delta\varphi_{\max}$ and $\Delta\varphi_{\min}$ are the maximum and minimum of $\Delta\varphi_i$, respectively. The phase shift $\Delta\varphi_{\text{bulk}}$ caused by bulk motion was obtained by locating the peak of the histogram

$$\Delta\varphi_{\text{bulk}} = \max[H(\Delta\varphi_i)], \quad -\pi < H(\Delta\varphi_i) < \pi \quad (4)$$

$\Delta\varphi_{bulk}$ is subtracted from its corresponding $\Delta\varphi_i$ to compensate for the bulk motion artifact for each line of the ODT image.

2.3 Scan patterns and eye movement compensation

The first scan pattern we used for the study is a set of evenly spaced concentric circles around the optic disc of the eye. This scan pattern was chosen to cover all major retinal arteries and veins. This scan pattern was used to test the algorithms for blood vessel detection. As illustrated in Fig. 1(a), the circular scan pattern consisted of 56 normal density (1024) and one high density (8192) depth scans (A-lines). The radius of the circles spanned evenly from 0.73 to 2.73mm on the fundus. The high density scan had a scan radius of 1.73mm, which is the same as that used in the commercial time-domain OCT machine for glaucoma imaging.[8], A donut shaped *en face* OCT fundus image [11] can be generated and registered on the corresponding fundus photograph for the same eye. By comparing the OCT fundus image and the fundus photograph arteries and veins can be recognized. An ODT image can be generated from the high density scan. The ODT image helps not only verify the accuracy of the calculation of the lateral coordinates of each recognizable blood vessel but also locate the depth coordinate of each blood vessel on the high density OCT image.

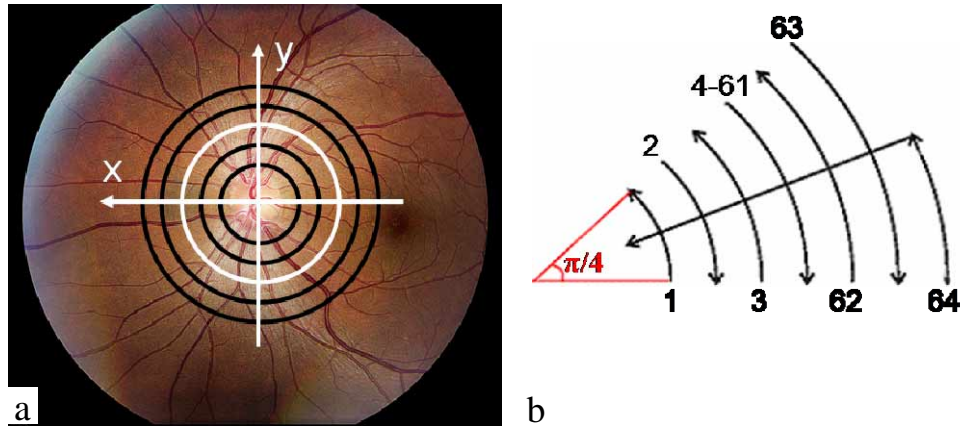


Fig. 1. (a). Circular scan pattern centered on the optic disk. The black circles represent the normal density scans (1024 A-lines); the white circle represent the high density scan (8192 A-lines). (b) Arc scan pattern. Scans 1,2,3,62,63 are used to calculate the Doppler angle. Scan 64 is used for alignment. Scans 4-61 were scanning the same area.

Another scan pattern we used is arc shaped [Fig. 1(b)] for imaging individual blood vessels. The scan pattern consisted of 63 concentric arcs, each of which has 1024 A-lines, subtending an angle of $\pi/4$ with a radius spanning from 1.48 to 1.98mm, and one depth alignment scan (reference scan, scan No.64) for eye movement compensation. 58 scans (scan No.4 to No.61) were repeated at a radius of 1.73 mm. This arrangement of the scans is used to calculate the Doppler angle and the flow dynamics. A Doppler image was calculated for each of the arc scans, therefore allowing accurate 3D coordinate calculations.

Also illustrated in Fig. 1(a) is the coordinate system we used for the entire study, where the X-axis represents the horizontal position, the Y-axis represents the vertical position, and the Z-axis represents the depth position. We also defined r ($1.48mm \leq r \leq 1.98mm$) as the scan radius and α ($0 \leq \alpha \leq 2\pi$) as the scan angle, both can be pre-determined by the scan data. For each pixel on the circular OCT image the lateral coordinates (x, y) can be calculated as $x = r \cos \alpha$ and $y = r \sin \alpha$.

Involuntary eye movements during image acquisition can cause distortions to the retinal OCT images as well as the locations of retinal vessels due to limited imaging speed, which in turn add an error to the Doppler angle calculation. The ultimate solution to this problem is to increase the imaging speed. With current commercially available cameras for the spectrometer, the space for improving imaging speed is very limited. As a result, compensation for the distortions caused by eye movements with post-processing is necessary. To compensate for the eye movements a linear fast reference scan crossing all the arc scans was added at the end of the arc scan. During the fast linear scan eye movement can usually be neglected, the linear scan provides a reference for all the arc scan images in the depth direction. The depth position for each arc scan can be adjusted according to this reference scan and thus provides compensation in the depth direction. Compensation according to the reference scan image can be done in different ways. In one method we can detect the front surface of all the images and each B-scan will be shifted in the Z direction according to the difference of the z coordinates of the surfaces between the B-scan and the reference image at the corresponding (x, y) position. We can also calculate the shift for each B-scan by means of the correlation coefficients between the corresponding A-lines in the circular and reference B-scans.

The blood vessels can be treated as straight lines in the small arc scan area. The Doppler angle can be calculated using the following relationship:

$$\cos \theta = \frac{\Delta z}{\sqrt{\Delta x^2 + \Delta y^2 + \Delta z^2}}, \quad (5)$$

Where Δx , Δy , and Δz are the projections of the vessel segment in the scanned area on the X, Y, and Z axes. By differentiation of Eq. (5) we have

$$d(\cos \theta) = \frac{-\Delta x \Delta z d(\Delta x) - \Delta y \Delta z d(\Delta y) + (\Delta x^2 + \Delta y^2) d(\Delta z)}{(\Delta x^2 + \Delta y^2 + \Delta z^2)^{3/2}}. \quad (6)$$

In retina imaging, θ is close to 90° and $\Delta z \ll \Delta x, \Delta y$. As a result, we can see from Eq. (6) the variation of the Doppler angle is more sensitive to the variation of Δz . So that compensation for eye movement in the z direction is the most important in calculating the Doppler angle.

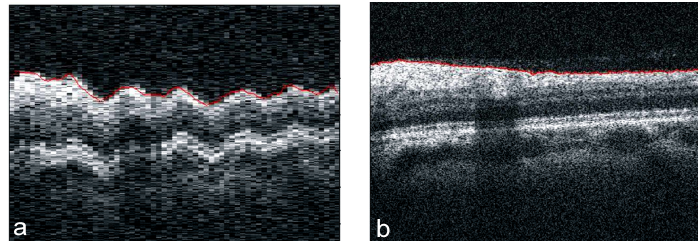


Fig. 2. (a). virtual B-scan extracted from the 3D data at the location of the reference scan. The red line shows the segmented ILM (inner limiting membrane) that is used for alignment. (b) The reference scan image.

Fig. 2 shows the extracted image (virtual B-scan) from the acquired 3D data corresponding to the positions of the linear reference scan together with the reference scan image. The inner limiting membrane (ILM) can be extracted by using our segmentation algorithm for both images. By comparing the Z coordinates at the same locations of the segmented ILM in both images, a compensation curve can be generated.

2.4 Automatic quantitative blood vessel detection

2.4.1 Automatic detection of lateral coordinates

To calculate the Doppler angle, the coordinates of the blood vessel need to be determined on each OCT cross sectional image. Our strategy is to first determine the lateral position and the diameter of each blood vessel on the cross sectional OCT intensity image and then determine the depth location of the vessel on the ODT image. In an OCT cross sectional image a blood vessel casts a shadow behind it, which exhibits as a low reflection region in the retinal fundus reflection graph. However, surface reflections can cause distortions to the blood vessel profile and add difficulty in blood vessel automatic detection. Other techniques were introduced to minimize the effect of surface reflection in retinal blood vessel detection. [12] Here we used our previously published method known as the shadowgram [11] to improve the retinal blood vessel profile and minimize the surface reflection effect. Using this technique we can generate a high contrast retinal reflection distribution called shadowgraph, where each vessel was characterized as a low reflection region.

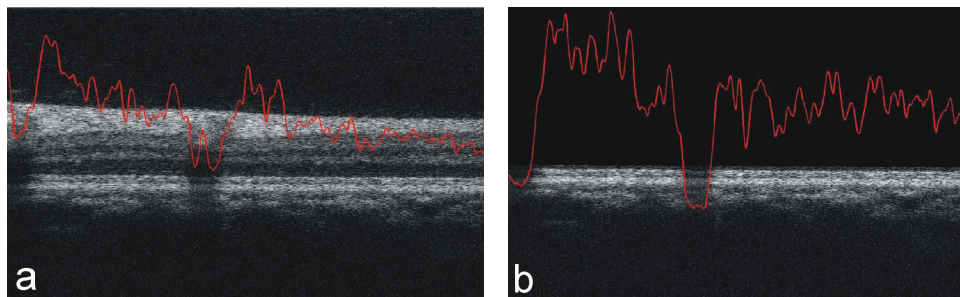


Fig. 3. Improved blood vessel profile using blood vessel shadowgraph. (a) Original B-scan image. (b) The B-scan image after the surface layer was removed. The calculated fundus reflection distribution corresponding to the B-scan and the fundus shadowgraph were superimposed on the images.

The shadowgraph was generated by first removing the surface layers of the retinal OCT image and then summing all the pixel intensity values along each A-scan. Fig. 3 shows the original OCT image, the image after the surface layer was removed, and the calculated reflection distributions (the vessel profiles). From the calculated fundus reflections we can see that not only the vessel contrast but also the vessel profile was improved by using the shadowgraph, which promises a more accurate detection of the vessel location and its diameter.

To extract the lateral coordinates the shadowgraph was first smoothed by using a smooth filter (Savitzky-Golay, length=3, weighing factor=21 in Matlab). The background was removed from the smoothed curve by subtracting the low pass filtered data. After normalization, thresholding according to a predetermined value was applied. The blood vessel locations and diameters were then determined.

2.4.2 Automatic detection of Depth coordinates

Automatically detecting the depth position of a blood vessel is much more challenging than detecting the lateral coordinates. Various methods may be used on either the intensity image or the ODT image. We first reported on the successful detection of the depth position of a blood vessel on an ODT image after the lateral coordinates and vessel diameter were determined. [6] The same method was used in the current study.

To detect the z coordinate of the center of a blood vessel, comprehensive information about the blood vessel was used, i.e. the lateral coordinates, the vessel diameter, and the Doppler shift caused by the blood flow. The basic idea is that outside the blood vessel the

calculated Doppler shift consists of only random noise where inside the vessel the Doppler shifts are correlated. Accordingly, a circular window filter moving in the z direction along the detected vessel position can be constructed. The diameter of the circular window should be equal or less than the diameter of the blood vessel. The filter can be either type of a function that examines the correlation of the values inside the window. The simplest type of the function is averaging.

We used an averaging filter for the detection of the z coordinate of a blood vessel. An average versus z curve was obtained for each blood vessel. A maximum or minimum will be reached, depending on the direction of the blood flow, when the center of the window coincides with the center of the blood vessel. Therefore, by locating the maximum or minimum of the average versus z curve the z coordinates of the center of a blood vessel can be determined.

Fig. 4 shows an example of the ODT image of a retinal blood vessel in an arc scan around the optic disc (a), the center of the blood vessel marked according to visual measurement (b), and the result of the moving circular window filtering. In this case, the location of the minimum corresponds to the center of the blood vessel. We can see from the figure that the moving circular window filtering worked well in locating the depth position of the vessel center.

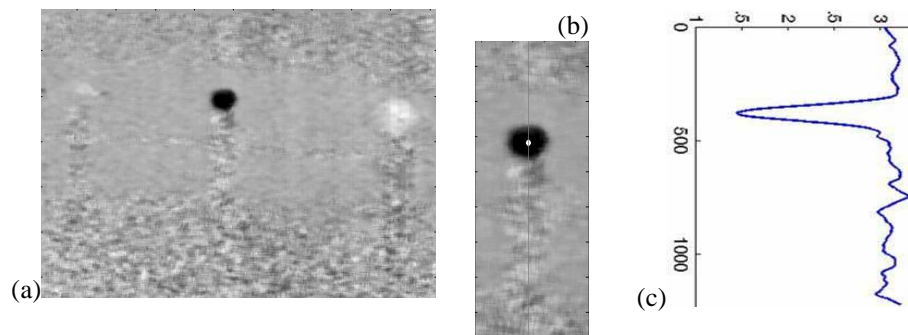


Fig. 4. Depth coordinate detection by using a circular window averaging. (a) The original ODT image of an arc scan; (b) The blood vessel center was marked by visual measurement; (c) Averaging curve along the direction of the A-line passing through the center of the blood vessel with a diameter of 60 pixels. Notice the position of the peak corresponds with the depth position of the center of the blood vessel.

Upon determination of the coordinates of a blood vessel the Doppler angle can be calculated by using Eq. (5). The absolute velocity of the blood flow inside the vessel can then be calculated. Knowing the absolute average velocity (\bar{v}_a , averaged across the vessel) of the blood flow and the vessel diameter (d), the blood flow rate (R) can be calculated as

$$R = \bar{v}_a \pi d^2 / 4 . \quad (7)$$

Fig. 5 illustrates the procedure for the data processing.

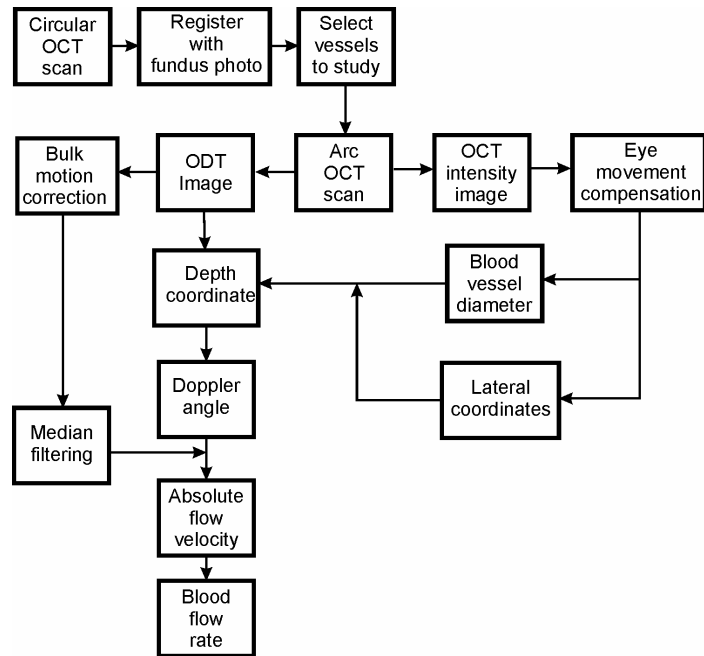


Fig. 5. Illustration of the procedure for calculation of the Doppler angle and the blood flow.

3. Results and discussion

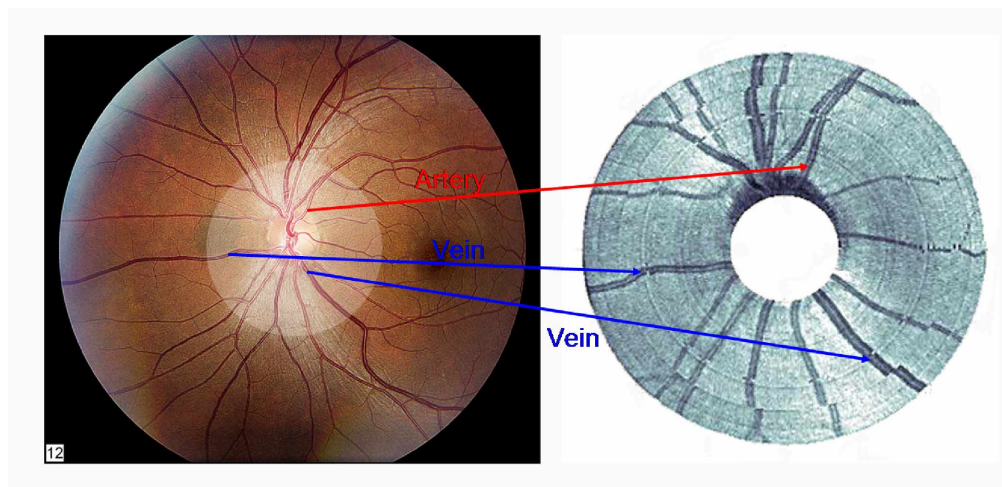


Fig. 6. Color fundus photograph of a normal human eye and the corresponding OCT fundus image generated from the circular scans around the optic disc.

The algorithms for detecting the vessel coordinates and diameters were applied to the measured data. Fig. 6 shows the re-constructed OCT fundus image from the circular scan around the optic disc and the corresponding color fundus photograph of a normal eye of a volunteer. By comparing both images retinal arteries and veins can be recognized on the OCT

fundus image. The OCT fundus image was used to determine the accuracy of the algorithm for the detection of the lateral position of the blood vessels. The OCT fundus image registered well with the fundus photograph. Fig. 7 shows the step-by-step data processing results and the detected vessel centers and vessel boundaries on the circular OCT and the ODT images.

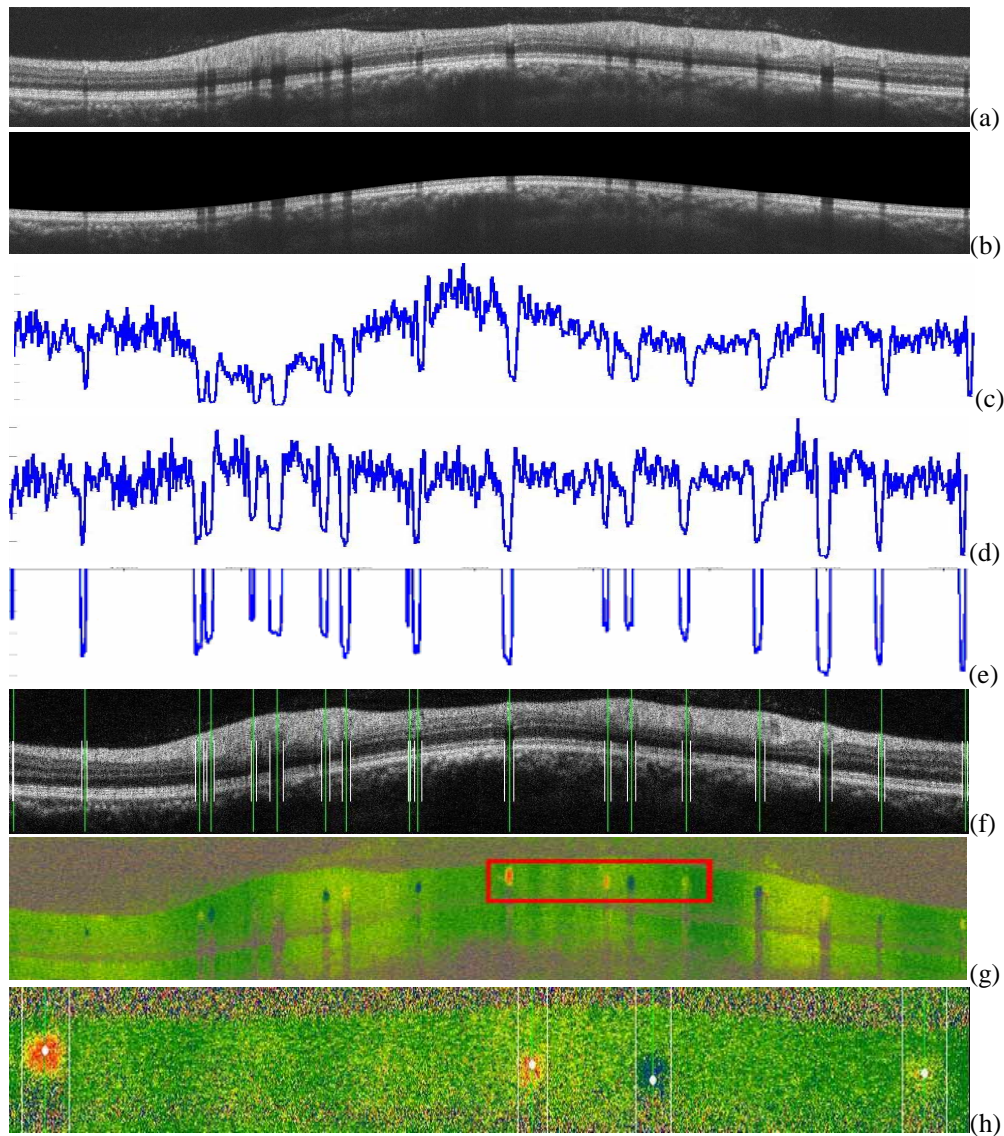


Fig. 7. (a). OCT image of a high density circular scan (8192 A-lines) around the optic disc of a normal human eye; (b). The OCT image after removal of the surface layers; (c). The original shadowgraph; (d). The shadowgraph after background correction and normalization; (e). the shadowgraph after thresholding; (f). Recognized blood vessel centers and boundaries are marked on the OCT image; (g). The ODT image for the same OCT scan; (h). Magnified view of the region marked in (g). where the calculated blood vessel centers are marked.

To test the accuracy of the algorithm the eyes of four normal volunteers were imaged and analyzed. We define the accuracy for the detection of the lateral coordinates as the percentage of the number of blood vessels automatically detected to the number of blood vessels detected

visually on the circular OCT fundus image. We achieved 100% accuracy for the eyes we have imaged. The accuracy for the detection of the depth coordinate was defined by comparing the visually determined blood vessel center on the Doppler image with the center determined by the algorithm (see Fig. 8 as an example). If the distance between the two centers was less than half of the radius of the vessel, we define it as a success. For the imaged normal eyes we achieved an accuracy of 84.4% for all the vessels. For large blood vessels (diameter larger than 50 pixels) depth positions were detected with an accuracy of 93.3%.

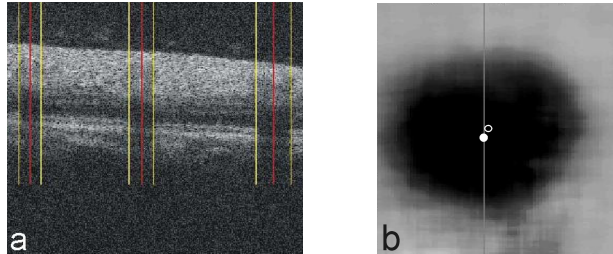


Fig. 8. (a). the detected vessel location and boundaries in an arc scan image; (b) comparing the automatically detected vessel center (solid circle) and the visually detected center (open circle) on the ODT image of a vessel.

The detected blood vessel coordinates contain the effect of eye movement. Before the vessel coordinates were used for calculation of the Doppler angle eye movement compensation was applied to the arc scans. After eye movement compensation linear fitting was used for the x, y, and z coordinates of the blood vessels. The angle of the fitted line in reference to the Z axis is the calculated Doppler angle. Fig. 9 shows the process and results for eye movement compensation for a blood vessel.

After calculation of the Doppler angle, the absolute blood flow velocity can be calculated. After the ODT image was median filtered the flow speed inside the blood vessel was averaged across the vessel for each time point to get the mean of the flow speed. One artery marked on Fig. 10(a) for a normal eye was studied. The calculated Doppler angle for this vessel is 87.8° . The calculated absolute velocity of the blood flow over time is shown in the curve of Fig. 10(b). The blood flow velocity over the time of measurement was calculated to be 30.4 ± 9.5 mm/s (mean and standard deviation). The standard deviation reflects pulsating behavior of the artery. The volunteer's pulse rate measured separately immediately after the OCT imaging was 58 pulses/min, which agrees with the velocity calculation in Fig. 10b. The diameter of the vessel in the measured region is $109 \mu\text{m}$. As a result, the average blood flow in this vessel is $17 \mu\text{l}/\text{min}$.

One vein marked on the fundus photograph shown in Fig. 11(a) for another normal eye was also studied. The calculated Doppler angle for this vessel is 87° . The calculated absolute flow velocity of the blood flow, averaged across the vessel, is shown in the in Fig. 11(b). The averaged blood flow velocity over the time of measurement was calculated to be 16.4 ± 3.9 mm/s (mean and standard deviation). The diameter of the vessel in the measured region is $51 \mu\text{m}$. As a result, the average blood flow in this vessel is $2.01 \mu\text{l}/\text{min}$.

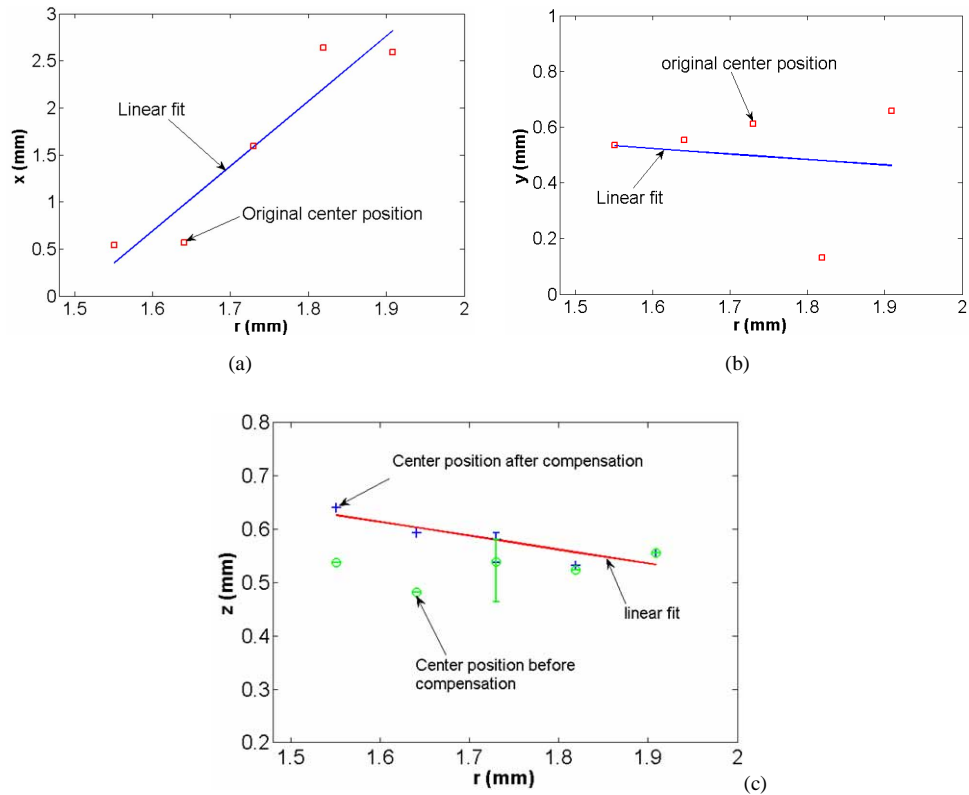


Fig. 9. The detected x , y , and z coordinates of the center of a blood vessel versus the scan radius r . Linear fitting were used for compensating variations of the x and y coordinates. The coordinates at $r=1.73$ mm are the average of the results of the 58 repeated arc scans. (a) x versus r ; (b) y versus r ; (c) z versus r before and after eye movement compensation. Also shown in (c) is the range of the z coordinates of the vessel center for the 58 repeated arc scans.

ODT images for the artery and vein are also shown in Fig. 10 and Fig. 11. During the alignment for imaging acquisition a real-time ODT image was displayed for the position at the repeated arc scan. The ODT image for the blood vessel of interest was optimized by adjusting the optical head of the OCT system, which is equivalent to adjusting the Doppler angle for the specific vessel. When the ODT image for one vessel was optimized the quality of the images for the other vessels also covered by the scan may be deteriorated. We speculate the reason for this deterioration is caused by that the Doppler angle was closer to 90° .

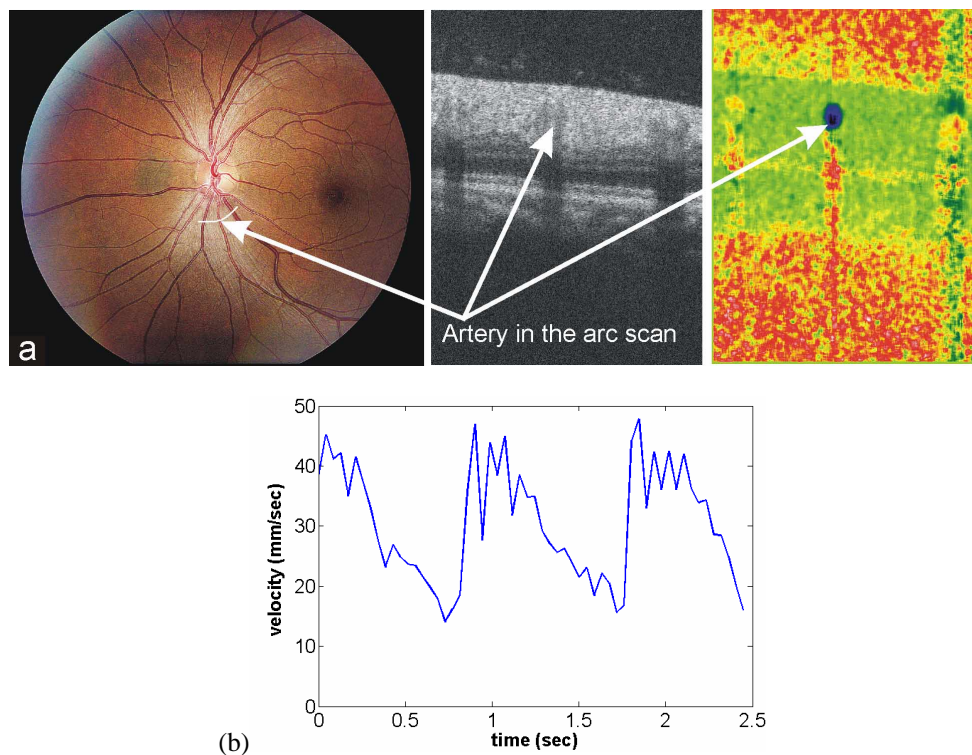


Fig. 10 The test result of an artery for a normal human eye. (a) The fundus photograph, the cross sectional OCT image at the position marked on the fundus photograph, and the ODT image. (b) The calculated absolute flow velocity averaged across the vessel area.

The calculated absolute velocity and flow rates for the artery and vein compared well with results obtained using other technologies.[13] The tests of the technique on current limited number of eyes were successful although more experiments are needed to test the accuracy and repeatability. Because the Doppler angles of retinal blood vessels are close to 90° , the error of the calculated absolute blood flow velocity is very sensitive to the error of the calculated Doppler angle. As analyzed in section 2.3 the Doppler angle is more sensitive to the eye movement in Z direction than that in X and Y directions, which is important considering that there is also no effective technique in the compensation for the movements in the X and Y directions. As a result, in our current technique eye movements in the X and Y directions were corrected only with linear fitting.

To test the accuracy of the calculation of the Doppler angle and the blood flow rate we measured the total flow rate of a vein before and after a bifurcation. Two measurements at the locations shown in Fig. 12 were taken. For the first measurement we scanned the area that contained the vein before bifurcation (parent vessel), while in the second measurement we scanned the area that contained both branches after bifurcation (daughter vessels). The time interval between the two measurements was about 15 minutes, during which the subject kept the same body position. The two measurements were taken at the same conditions where the room was kept dark to minimize the outside influence to the blood flow. The results of the measurements are shown in Table 1. The calculated average blood flow entering the bifurcation from the two branches was $2.23 \mu\text{l}/\text{min}$ while the average blood flow leaving the bifurcation was $2.17 \mu\text{l}/\text{min}$. The result provided good validation of our technique for the calculation of the Doppler angle and the blood flow rate. We are planning to build a phantom

simulating a blood vessel with adjustable 3D orientation and flow rate to further test the accuracy of our algorithm.

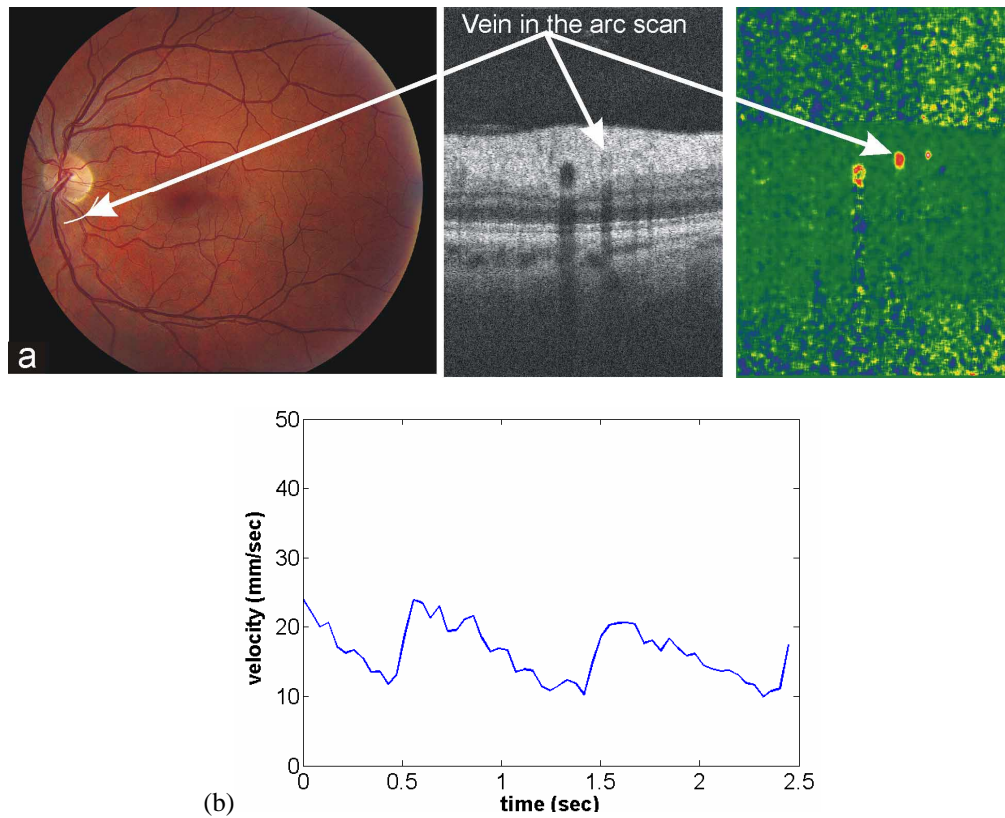


Fig. 11. The test result of a vein for a normal human eye. (a) The fundus photograph, the OCT cross sectional image at the position marked on the fundus photograph, and the ODT image. (b) The calculated absolute flow velocity averaged across the vessel area.

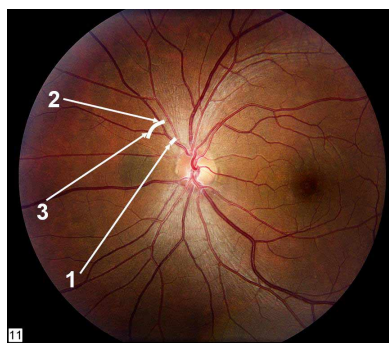


Fig. 12. Color fundus photograph of a normal human eye with markers indicating the location of the scan areas. Vessel 1 corresponds to the vein before bifurcation, while vessels 2 and 3 represent the vessel branches after bifurcation.

Table 1. Calculated parameters of the vessels shown in Fig. 12.

Vessel #	1	2	3
Diameter (μm)	103	66	54
Velocity (mm/sec)	4.3	8	4.12
Doppler Angle	81.6°	83°	76.3°
Flow ($\mu\text{l}/\text{min}$)	2.17±0.57	1.65±0.23	0.58±0.07

4. Conclusion

Doppler angle of retinal blood vessels including arteries and veins were successfully calculated by using the comprehensive information provided by high speed SD-OCT—structural information from the OCT intensity image and speed information from the ODT image. The lateral coordinates of a blood vessel can be extracted accurately by using the technique of blood vessel shadowgram, which not only enhanced contrast of the blood vessel against the reflecting background but also improved the vessels profile. The depth coordinate of a blood vessel was calculated by using a moving circular window filter in the ODT image after the lateral coordinates and the vessel diameter were extracted. By calculating the Doppler angle of a blood vessel the absolute blood flow velocity and the blood flow rate and be calculated. The technique was successfully tested on retinal arteries and veins for normal human eyes.

Acknowledgments

The authors thank Robert Knighton and Xiangrun Huang from Bascom Palmer Eye Institute University of Miami Miller School of Medicine for their support. This study is supported in part by the NEI P30 Core Grant Ey014801 and U.S. Army Medical Research and Materiel Command (USAMRMC) grant W81XWH-07-1-0188.